Spectrum-Control of Poly(p-phenylene vinylene) Nanofibers Fabricated by Electrospinning with Highly Photoluminescent ZnS quantum dots

Shuhong Wang[1], Zhiyao Sun[1], Eryun Yan[2,*], Liguo Sun,[1]Nan Huang[1], Weilin Zang[1], Liang Ni[1], Qinggui Wang[1,3,*], Yang Gao[1], Xiankai Jiang[1], Xuduo Bai[1], Feng Tang[1]

[1] Key Laboratory of Functional Inorganic Material Chemistry (School of Chemical Engineering and Material, Heilongjiang University), Ministry of Education, 150080, P.R. China
[2] College of Materials Science and Engineering, Qiqihar University, Qiqihar 161006, P.R. China
[3] College of Agricultural Resource and Environment, Heilongjiang University, Harbin, 150080, P.R. China
[*]E-mail: openair@163.com, yaney359@126.com

ZnS quantum dots(QDs) with excellent fluorescence properties have been incorporated into poly(p-phenylene vinylene)(PPV) nanofibers by the electrospinning method without any intermediate, and they were well dispersed inside the nanofibers homogeneously with lesser aggregation. ZnS QDs and the composite nanofibers were characterized morphologically and optically by scanning electron microscopy(SEM), transmission electron microscopy(TEM) and photoluminescence(PL) measurements. The average diameter of the hybrid fibers was 167 nm and the average size of ZnS QDs was 3.8 nm. The peaks of the PL and UV-vis absorption spectra of the as-prepared PPV/ZnS QDs composite nanofibers were blue shifted compared to pure PPV nanofibers.

1. INTRODUCTION

Electrospinning is a very facile and feasible method for fabricating nanofibers [1]. In addition to its simplicity and low-cost, it was a versatile method to control the surface properties of the nanostructures and the supramolecular assembly of the polymer molecules within the fibers [2]. Under high strain rate, orientation of polymer molecules along the fiber longitudinal axis can be observed [3]. Via the electrospinning technology, anisotropic shapes and molecular assemblies can be obtained,

therefore, the method well suited for the fabrication of nanofibers with conjugated systems. Conjugated polymer electrospun(ES) fibers showed distinct electronic and optoelectronic properties as compared with films due to the geometrical confinement of electrospinning process [4].

Conjugated polymers have received continued research interest for the last 30 years [5]. Poly(phenylene vinylene)(PPV) is a kind of typical conjugated polymer with excellent properties, such as photovoltage(PV) [6], electroluminescence(EL), photoluminescence(PL) and non-linear optical properties [7, 8]. As a kind of hole transport material, PPV has wide range of applications in organic photovoltaic devices[9] and optoelectronic devices [10]. Many works have been focused on the tuning of their fluorescent emission colors with the purpose of applying the conjugated polymers in the fields of full-color or white displays [11], cell imaging [12] and sensing [13], etc. Up to now, there are approximately several methods to tune PPV emission range: (1) One general method is to introduce different fluorophores into PPV by physical blending [14, 15]. However, in the case of physical blending, fluorescent instability may change due to the possible phase separation. (2) Another more effective way to tune the emission color of the PPVs is through chemical modification. Synthesizing PPVs with substituents having different electron-withdrawing or electron-donating features significantly changed the HOMO/LUMO level, consequently the band gap and the emission wavelength [16, 17]. (3) Adjusting the conjugation length or the extent of π-conjugation of the polymer backbone by synthesizing copolymers containing PPV moieties and some functional groups make possible to tune the emission range [18]. But complicated synthetic procedures were often required to alter the chemical structures of the polymer backbone and the side groups. Moreover, accurate control of the conjugation length is also very difficult. (4) Blending PPV or their derivatives with inert polymer such as polyvinyl alcohol(PVA), polyethylene oxide(PEO), poly(vinyl pyrrolidone)(PVP) or polymethacrylate(PMMA), but the luminescence quantum efficiency of the blend fibers was decreased [19]. (5) The incorporation of CdTe nanoparticles into the PPV precursor solution, and then blend the mixture with PVA to prepare films [20] or nanofiber [21]. However, introducing the inert polymer PVA as an intermediate will affect PPV's optoelectronic property.

In this work, we fabricated a kind of light-emitting electrospun composite nanofibers from water-soluble conjugated polymer PPV and ZnS QDs in a green and straightforward way in order to get spectrum-tuned PPV nanofibers. We synthesized ZnS QDs capped with carboxylated molecules with high luminescence in one single step. As is known, PPV precursor aqueous solution itself is difficult to be electrospun into uniform nanofibers without any intermediate, but uniform nanofibers can be obtained by controlling PPV precursor aqueous solution's content strictly. PPV/ZnS QDs composite nanofibers have excellent optical and photoelectric properties and have potential applications in photoelectric devices.

2. EXPERIMENTAL

2.1 Materials.

Tetrahydrothiophene and p-xylylene dichloride were purchased from Tokyo Chemical Industry Co. Ltd. Methanol, acetone, zinc nitrate($Zn(NO_3)_2$), sodium sulfide(Na_2S), tetrapropylammonium

hydroxide[(CH$_3$CH$_2$CH$_2$)$_4$]NOH and 3-Mercaptopropionic acid(MPA) were all obtained from Sinopharm Chemical Reagent Co. Ltd. All the chemicals were used as received without further purification.

2.2 Synthesis of Thiol-stabilized ZnS QDs.

The water-soluble photoluminescent MPA-capped ZnS QDs have been synthesized using 3-Mercaptopropionic acid as the stabilizer according to Ref. [22]. In brief, Zn(NO$_3$)$_2$ solution(0.04 M) and Na$_2$S solution(0.02 M) were prepared in deionized water. For the MPA/Zn^{2+}/S^{2-} ratio of 8:4:1, 1.28 mmol of MPA was added to 72 mL of deionized water and it was stirred for 5 min. Then 4 mL of Zn(NO$_3$)$_2$ solution was dropped slowly into the MPA solution with continuous stirring for 10 min. The pH value of the mixture was adjusted by adding the tetrapropylammonium hydroxide [(CH$_3$CH$_2$CH$_2$)$_4$]NOH until the pH value was 12, and it was stirred for 10 min. After that, 8 mL of Na$_2$S solution was added quickly with vigorous stirring to precipitate ZnS nanoparticles. 5 min was permitted for the ZnS nanoparticles to form and grow up, then another 12 mL of Zn(NO$_3$)$_2$ solution was added and it was kept stirring for another 5 min. The obtained thiol-stabilized ZnS QDs suspension was clear and colorless. After that, the mixture was divided into two parts. One was dialyzed against deionized water in order to remove ions, which was obtained for TEM and PL characterization and for preparing electrospinning solution. The other was dropped into ethanol with vigorous stirring to precipitate ZnS QDs and the QDs were washed repeatedly with ethanol until the system was neutral, followed by centrifugation and air drying at 50℃. The powder sample was obtained for XRD characterization.

2.3 Preparation of PPV Precursor.

The PPV precursor was prepared according to Wessling's synthetic route [23] and the optimized conditions provided by Halliday and co-workers [24]. PPV precursor aqueous solution was dialyzed in water for a week to remove ions, and then it was placed in a ventilated place for a week to remove the water. As a result, the thick aqueous solution of PPV precursor was obtained.

2.4 Preparation of PPV and PPV/ZnS QDs Spin Solutions.

A series of pure PPV precursor aqueous solutions with different concentration were prepared. The condensed ZnS QDs aqueous solution was added into PPV precursor solution under stirring for 20 min, until the solution became homogeneous and it was ultrasonically treated for 10 min before electrospinning. The content of ZnS QDs was about 4 wt.% in the PPV precursor solution.

2.5 Pure Polymer and Nanocomposite Fiber Fabrication.

The ES fibers were prepared using a single-capillary spinneret. The solution was loaded into a

10 mL syringe equipped with a stainless steel needle with inner diameter of 0.8 mm. The metallic needle was connected to a high-voltage power supply. The spin solution was continuously supplied at a flow rate of 0.5 mL/h using a syringe pump. These solutions were electrospun under an applied potential of 13 kV at a fixed collection distance of 15 cm. All the experiments were carried out at room temperature. In the case of preparing non-woven ES fibers, aluminum foil or quartz substrate, copper grids sticked on the aluminum foil were used as the nanofiber collector. The PPV precursor nanofibers were consequently thermally converted into PPV nanofibers at 20℃ under nitrogen for 15 min and then at 220℃ for 30 min to make those structures insoluble in most solvents (polar and organic).

2.6 Characterization.

The morphology of the nanofibers was characterized via a field-emission scanning electron microscopy(FE-SEM, MX2600FE). The inner microstructure of the nanofibers and the crystal structure of the resultant ZnS QDs were characterized with transmission electron microscope(TEM, FEI TECNAI F20) with an accelerating voltage of 80 kV. The dialyzed ZnS QDs suspension was dropped on the surface of a TEM grid with an ultra-thin carbon film. The FT-IR spectra were recorded on a Nicolet Avatar 360 FT-IR spectrometer using KBr pellet method in the range of 400~4000 cm^{-1}. A combined stead state fluorescence and phosphorescence lifetime spectrometer(FLSP920) was used to obtain the PL spectra of the as-spun nanofibers and the excitation wavelength was 470 nm. The fluorescence emission was collected in the range of 450~700 nm.

The fluorescence microscope photographs of the nanofibers were taken from a fluorescence microscopy(TE2000-U). UV-vis absorption spectra were collected using an ultraviolet spectrophotometry(Varian Cary 500, USA). X-ray diffraction(XRD, D8 advance) studies were performed to investigate the crystallization of ZnS QDs.

3. RESULTS AND DISCUSSION

3.1 ZnS QDs Analysis.

Figure 1 showed the TEM image of the synthesized ZnS QDs. As can be seen, the mean particle size of ZnS nanoparticles was in the range of 3-5 nm, and they were well dispersed and nearly spherical crystallites with clear lattice fringes. The fringe spacing of 0.22 nm corresponded to the (220) cubical zinc blende interplanar [25]. The inset section was selective-area electron-diffraction(SAED) pattern and it showed two electron diffraction rings, corresponding to (111) and (220) crystal plane. But the electron diffraction ring of (311) crystal plane can not be seen in the SAED. At the beginning of the crystal growth, the crystal structure was not complete, and the periodic structure of the crystals area was small. The conditions satisfying Bragg diffraction signal were less. If the intensity was small to a certain extent, the diffraction rings would be missing and the corresponding diffraction peak (2θ=56.70°) may be weak in the XRD patterns.
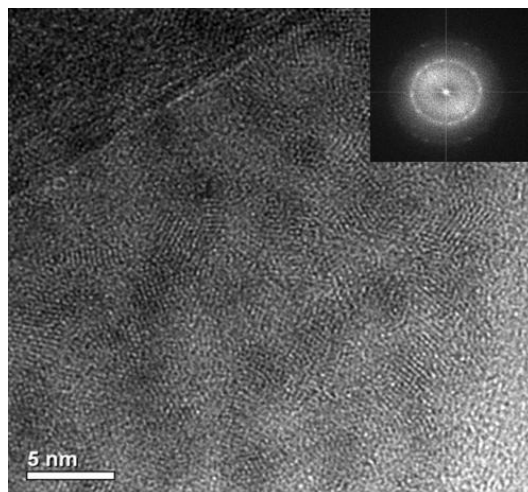
Figure 1. HR-TEM image of ZnS QDs.

Figure 2 showed the XRD patterns of the ZnS QDs. The wide angle XRD patterns for the ZnS QDs powder sample exhibited three distinct peaks in the range of $2\theta=20\sim70°$, which were the characteristic peaks of the cubic structure of ZnS. The three peaks appeared at angles (2θ) of 28.28°, 47.87° and 56.70° corresponding to the (111), (220) and (311) planes, which indicated that the QDs had a cubic zinc blende crystalline structure(JCPDS 05-0566). This was well in agreement with Ref. [26].
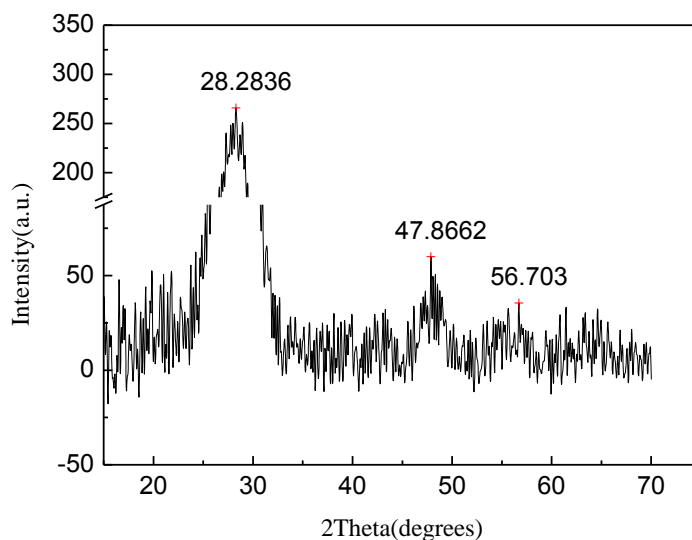

Figure 2. XRD patterns of ZnS QDs powder.

The peak intensity decreased, while the full width of the peak increased, indicating the low crystallinity and small crystallite size. It can be predominantly attributed to the short aging time and the existence of MPA, which affected the crystal size and crystallinity. In addition, it was also clearly observed that the diffraction peaks of ZnS exhibited slight movement compared with the standard

diffraction index. This may be due to the fact that the synthesized ZnS ODs were thiol-stabilized under the pH value of 12. Under this situation, thiol may coordinate with Zn^{2+}, and Zn-S-R complexes were analogous to a shell. The existence of organics may impact the crystallization of ZnS QDs obviously. The average crystallite size D, calculated using the Debye-Sherrer equation $D=K\lambda/(\beta cos\theta)$, was roughly about 3.8 nm based on the main peak (111), which was in agreement with the results of the TEM analysis (Figure 1).

The UV-visible absorption spectrum and the corresponding PL emission spectrum of the MPA-capped ZnS QDs aqueous solution were shown in figure 3. The absorption edges of the ZnS QDs were around 320 nm while the emission peak wavelength was at 412 nm, which was consistent with the blue light observed from the digital photo(insert of Figure 3). The emission peak wavelength of all the samples was about 100 nm larger than their corresponding absorption edge wavelength. This indicated that the emissions of the present ZnS QDs were trap-state emissions associated with electron transitions between the trap states and the conduction band(or valence band).
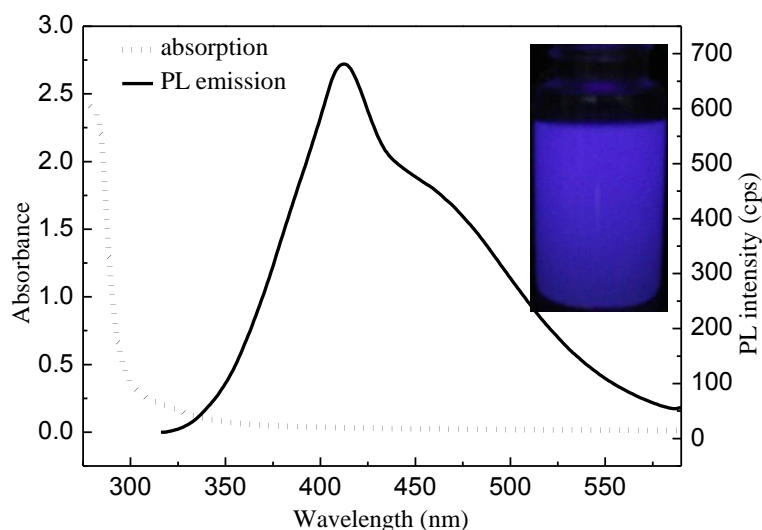

Figure 3. UV absorption and PL emission spectra of ZnS QDs aqueous solution (insert part is the digital photo of ZnS QDs under UV lamp with the excitation wavelength of 302 nm).

3.2 PPV/ZnS QDs Composite Nanofibers Analysis.

3.2.1 PPV Concentration *Selection.*

In fact, the concentration of polymer is the key factor influencing the viscosity of the solution, which plays an important role in the process of electrospinning. Meanwhile, the concentration is the most significant factor for controlling the diameter of fibers in the electrospinning process. PPV precursor aqueous solution is difficult to be electrospun relative to PVA and PVP solutions, which can be electropun into nanofibers only on a small concentration scope. By electrospinning, the pure PPV precursor aqueous solutions with different concentration were fabricated into nanofibers, and the concentration of 1.0 wt.% was selected as the optimal one. When the concentration was low($<$1.0

wt.%), beads-on-string structure was observed. With a higher solution concentration(1.0 wt.%), smooth fibers were obtained. When the concentration was increased further to 1.5 wt.%, nanofibers with large and nonuniform diameters were obtained, and the electrospinning process was very slow due to the high solution viscosity. Therefore, PPV precursor aqueous solution with the concentration of 1.0 wt.% was chosen for electrospinning of PPV/Zn QDs composites. Figure 4 shows the morphology of fibers obtained from pure PPV precursor aqueous solutions, indicating that the morphology of the electrospinning nanofibers depends strongly on the concentration of the polymer solution.
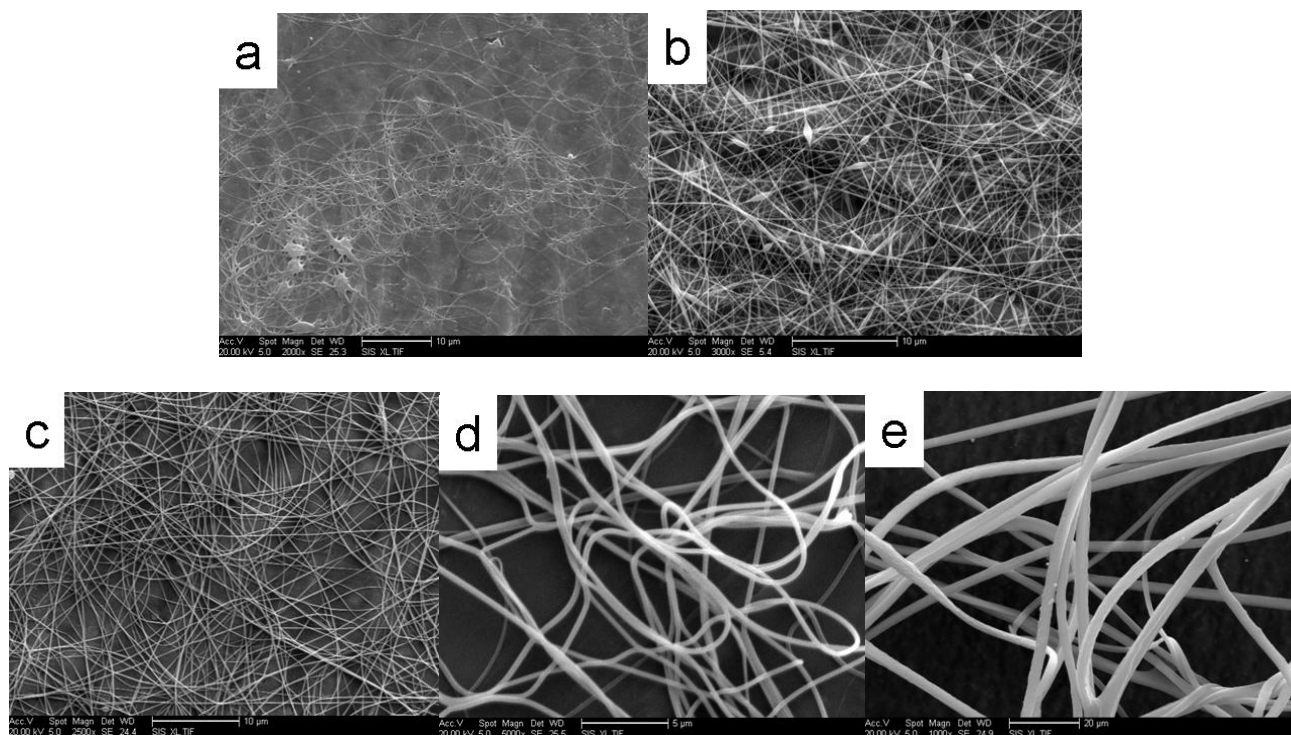

Figure 4. SEM images of PPV nanofibers with different concentration: (a) 0.5 wt.%, (b) 0.8 wt.%, (c) 1.0 wt.%, (d) 1.5 wt.% and (e) 2.0 wt.%.

*3.2.2 Morphology of PPV/ZnS QDs composite nanofibers.*

Figure 5 shows the typical FE-SEM images of pure PPV and PPV/ZnS QDs composite electrospun nanofibers. All the nanofibers with smooth surface were randomly oriented. Pure PPV nanofibers were homogeneous and continuous with an average diameter of 199 nm(Figure 5a). After the introduction of ZnS QDs, the average diameter of the PPV/ZnS QDs nanofibers with smooth surface decreased to 167 nm(Figure 5b). Because the particle size of the ZnS QDs was so small comparing to the nanofibers that we cannot observe the ZnS QDs on the surface of the composite fibers. The addition of ZnS QDs in the nanofibers had an important effect on the diameter of the composite nanofibers(the diameter decreased from 199 nm to 167 nm). This phenomenon can be explained that the addition of ZnS QDs increased the electric conductivity of the electrospinning solution. High conductivity resulted in sufficient elongation of a jet by the electrical force,

consequently produced thinner nanofibers [27]. And it was known that the higher amount of excess charge in the electrospinning jet would result in the smoother nanofibers.
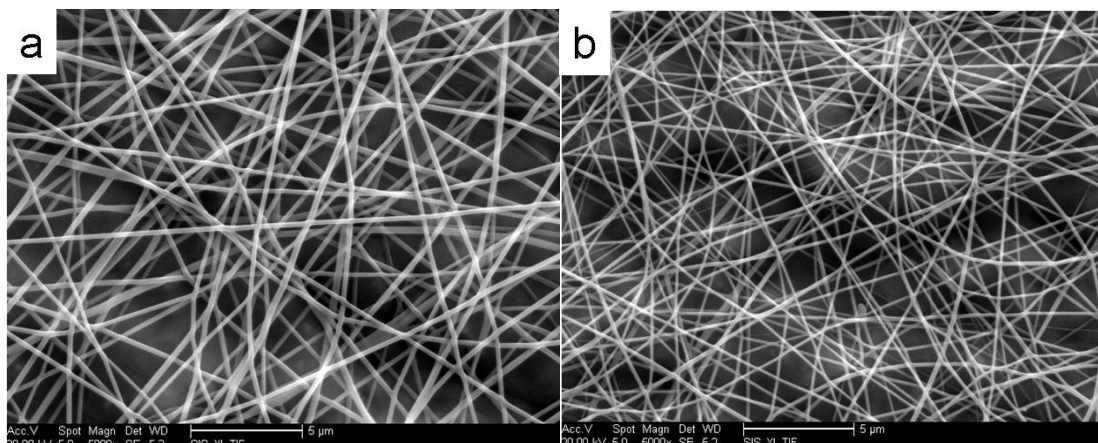
Figure 5. SEM images of the nanofibers: (a) pure PPV and (b) PPV/ZnS QDs.

The interior morphology and the ZnS QDs dispersion in the composites were investigated by TEM, presented in Figure 6. The ZnS QDs with uniform dispersion in the composite nanofibers were observed from the TEM image and their average diameter was only a few nanometers, which demonstrated that the wet mixing method we adopted was highly efficient and the inorganic nanoparticles can implement uniform dispersion in the fibers.
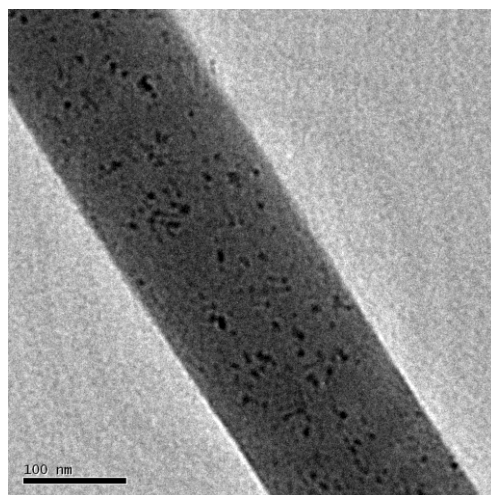

Figure 6. TEM image of the as-prepared PPV/ZnS QDs nanofibers.

As can be seen, there was very little agglomeration of ZnS QDs in the composite nanofibers. This agglomeration in spin solution was also favorable in energy as the Vander waals interaction

among the ZnS QDs was stronger compared with the weak interaction between ZnS QDs and PPV precursor. But once the composite nanofibers were formed, the agglomeration would not take place. Surrounded by PPV molecules, ZnS QDs had no chance to aggregate. PPV matrix provided a stable chemical environment for the ZnS QDs, and ZnS QDs dispersed homogeneously in the polymer matrix without reunion, expressing its size effect sufficiently.

3.2.3 UV-vis Absorption Spectra Analysis.
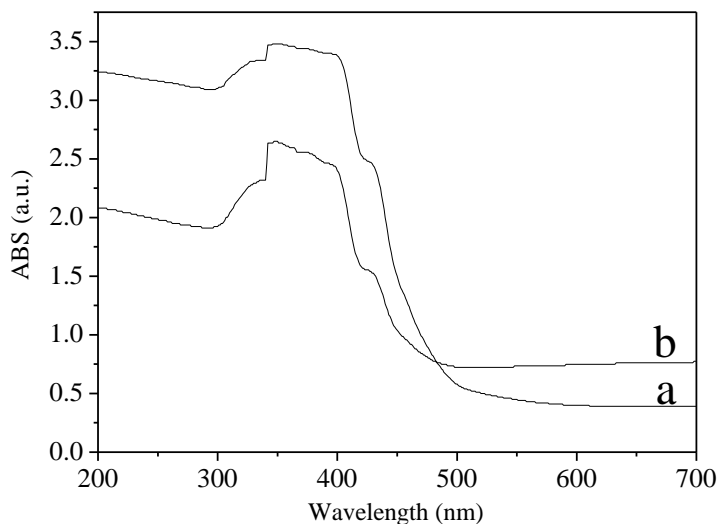
Figure7. UV-vis absorption spectra: (a) pure PPV nanofibers and (b) PPV/ZnS QDs composite nanofibers.

Figure 7 presented the UV-vis absorption spectra of the nanofibers in the wavenumber ranging from 200 to 700 nm. Both the UV-vis absorption spectra showed a relatively strong absorption band from 300 to 450 nm and this was attributed to the p-p* transition of the PPV component [28]. The absorption peak of PPV fibers was slightly broader than that of the PPV/ZnS QDs composite fibers. The PPV/ZnS QDs composite nanofibers(Figure 7b) exhibited a blue-shift compared to pure PPV nanofibers (Figure 7a), revealing the reduced conjugation length along the polymer backbone [29]. This may produce the interaction between PPV molecular and ZnS QDs and degrade the p-conjugated polymer backbone or it was attributed to the weakening of the intermolecular force between PPV chains after introducing ZnS QDs [30].

3.2.4 Fluorescence Spectra Analysis.

In order to contrast the luminescence characteristics of the pure PPV nanofibers and PPV/ZnS QDs composite nanofibers, PL spectra were investigated. The excitation wavelength was 470 nm. Figure 8a and 8b showed the PL excitation spectra of the pure PPV and PPV/ZnS QDs nanofibers, respectively. As shown in Figure 8a and 8b, the maximum excitation wavelength of PPV nanofibers

was at 469 nm, while that of the PPV/ZnS QDs composite nanofbers was at 450 nm. There was a blue-shift of 19 nm, corresponding well with the UV-vis absorption results.

Figure 8c and 8d showed the PL emission spectra of the pure PPV and PPV/ZnS QDs composite nanofibers, respectively. Pure PPV nanofibers emitted yellow-green fluorescence at about 542 nm with two vibronic side-bands, which were assigned to 0-1, 0-0 and 0-2 transitions [31]. The emission peak originated from the 0-0 transition of these fibers was observed at 513 nm and 0-1 peak was at 542 nm. As shown in Figure 8d, for PPV/ZnS QDs composite nanofibers, the emission peak of 0-0 and 0-1 phonon bands were at 494 nm and 524 nm, respectively. The emission spectra shape of the pure PPV nanofibers and PPV/ZnS QDs composite nanofibers was basically same, but there was a blue-shift in the emission spectrum of PPV/ZnS QDs composite nanofibers. It is well known that polymer luminescent material emission peak position is determined by the band gap of the π-π* transition, which is a function of the structure of PPV and modifications with any specific purpose will affect the band gap and consequently the peak position [32]. The blue-shift may be attributed to several reasons: the interaction between PPV molecular and ZnS QDs occured when the thermal treatment was conducted under inert atmosphere, which degraded the p-conjugated polymer backbone; the intermolecular force between PPV chains was weakened after introducing ZnS QDs, which decreased the effective conjugated length; the reabsorption by neighboring chains of the emitted light that originated from the 0-0 transition was reduced because the PPV/ZnS QDs composite nanofibers consisted of fewer polymer chains in comparison with pure PPV nanofibers and there was much interchain contacts between the polymer chains; slight Fluorescence Resonance Energy Transfer(FRET) [33]. At present we do not have enough data to select among them.
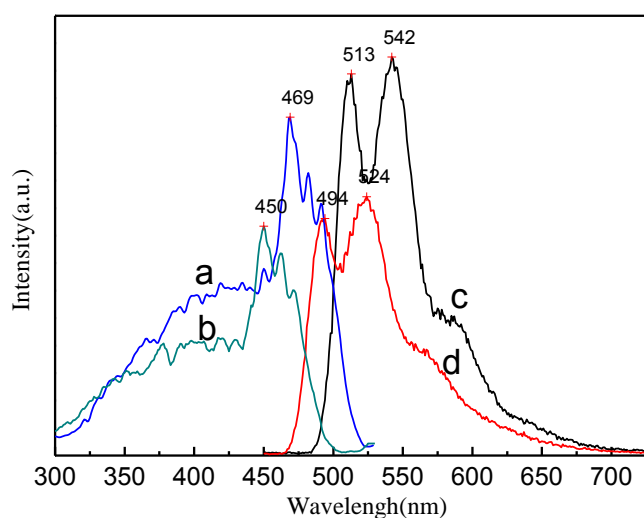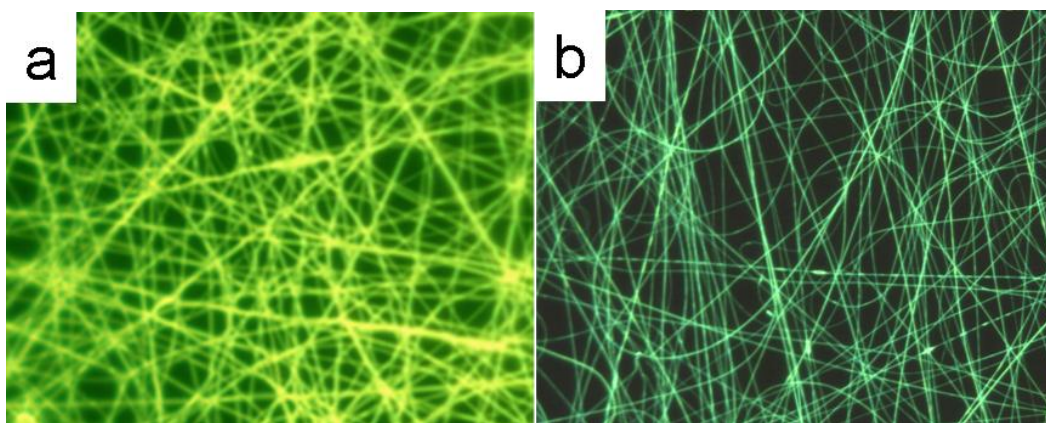

Figure 8. Fluorescence spectra of PPV nanofibers and PPV/ZnS QDs composite nanofibers.

3.2.5 Fluorescence Photos Analysis

Figure 9 showed the fluorescence microscope photographs of the nanofibers. It was clearly seen that all the nanofibers were random and they were more than several millimeters in length. In

addition, the diameter of the composite nanofibers was thinner than that of the pure PPV nanofibers. The morphology and distribution of fibers was in accordance with the results of the SEM images. As shown in Figure 9a, pure PPV nanofibers emitted bright yellow-green fluorescence. Due to the smaller size of ZnS QDs comparing with PPV nanofibers and the strong fluorescence intensity of PPV, ZnS QDs fluorescence was overshadowed by the strong fluorescence PPV. So we cannot observe the fluorescence of ZnS QDs obviously from the fluorescence microscope photograph in Figure 9b. Whereas with the addition of ZnS QDs, PPV/ZnS QDs composite emitted strong green fluorescence, that was, the fluorescence color of nanofibers had obviously changed. At the same time, we cannot observe the particles clearly in the composite fibers because ZnS QDs were small and well dispersed in the composite fibers without big agglomeration, which was consistent with the TEM analysis.

Figure 9. Fluorescence microscope photographs of (a) pure PPV nanofiers and (b) PPV/ZnS QDs composite nanofibers.

4. CONCLUSIONS

Aqueous MPA-stabilized ZnS QDs with high fluorescence quality were successfully synthesized. Their emission peak was at 412 nm and the grain size was 3.8 nm. Without any intermediate, the PPV/ZnS QDs composite nanofibers were fabricated by electrospinning. The SEM results showed that the composite nanofibers were homogeneous and continuous with an average diameter of 167 nm. Fluorescence spectra and fluorescence microscope photographs analysis indicated that the spectrum of the composite nanofibers took place obvious blue-shift in contrast to pure PPV nanofibers. It provided a feasible thought by introducing quantum dots into the luminescent material to shift the emission position and intensity. This hybrid photoluminescent nanomaterial made preparation for further fabrication of the photoelectric devices such as polymer light-emitting diodes (PLEDs), flat panel displays and photovoltaic devices.

References

1. A. Greiner and J. H. Wendorff, *Angew. Chem. Int. Ed.*, 46 (2007) 5670-5703.
2. K.Z. Yin, L.F. Zhang, C.L. Lai, L.L. Zhong, S. Smith, H. Fong and Z.T. Zhu, *J. Mater. Chem.*, 21 (2011) 444-448.
3. Z.Y. Li, H.M. Huang and C. Wang, *Macromol. Rapid Commun.*, 27 (2006) 152-155.
4. C.C. Kuo, C.H. Lin and W.C. Chen, *Macromolecules*, 40 (2007) 6959-6966.
5. W. Zhao, J. Song, Y. Shao, W. Zhang, A. Au and L.J. Fan, *Macromol. Chem. Phys.*, 213 (2012) 1913-1921.
6. Z.H. Huang, J.H. Yang, L.C. Chen, X.J. Wang, W.L. Li, Y.Q. Qiu, J.T. Zhang and R.S. Wang, *Synth. Met.*, 91 (1997) 315-316.
7. J.H. Burroughes, D.D.C. Bradley, A.R. Brown, R.N. Marks, K. Mackay, R.H. Friend, P.L. Burns and A.B. Holmes, *Nature*, 347 (1990) 539-541.
8. T.E. Mates, C.K. Ober and R. Norwood, *Chem. Mater.*, 5 (1993) 217-221.
9. S. Günes, H. Neugebauer and N.S. Sariciftci, *Chem. Rev.*, 107 (2007) 1324-1338.
10. Y. Jin, S. Song, S.H. Park, J.A. Park, J. Kim, H.Y. Woo, K. Lee and H. Suh, *Polymers*, 49 (2008) 4559-4568.
11. J.S. Huang, G. Li, E. Wu, Q. F. Xu and Y. Yang, *Adv. Mater.*, 18 (2006) 114-117.
12. P. Howes, M. Green, J. Levitt, K. Suhling and M. Hughes, *J. Am. Chem. Soc.*, 132 (2010) 3989-3996 .
13. S.W. Thomas, G.D. Joly and T.M. Swager, *Chem. Rev.*, 107 (2007) 1339-1386.
14. N. Mizoshita, Y. Goto, T. Tani and S. Inagaki, *Adv. Mater.*, 21 (2009) 4798-4801.
15. H. Mochizuki, T. Mizokuro, X. Mo, N. Yamamoto, N. Tanigaki and T. Hiraga, *Thin Solid Films*, 499 (2006) 410-414.
16. H.J. Cho, D.H. Hwang, J.D. Lee, N.S. Cho, S.K. Lee, J. Lee, Y.K. Jung and H.K. Shim, *J. Polym. Sci., Part A: Polym. Chem.*, 46 (2008) 979-988.
17. S.J. Yoon, S. Samal and T.H. Yoon, *Eur. Polym. J.*, 46 (2010) 2282-2289.
18. M. Mbarek, F. Massuyeau and J. L. Duvail, *J. Appl. Polym. Sci.*, 130 (2013) 2839-2847.
19. H.C. Chen, C.L. Liu, C.C. Bai, N.H. Wang, C.S. Tuan and W.C. Chen, *Chem. Phys.*, 210 (2009) 918-925.
20. H. Wei, H. Sun , H. Zhang, C. Gao and B. Yang, *Nano Res.*, 3 (2010) 496-505.
21. Z.Y. Sun, Y. Xie, C. Wang, L.G. Sun, S.H. Wang, L. Ni, P.F. Yan, Y. Gao, L.L. Zang, D.S. Lu and G.Q. Xu, *Int. J. Electrochem. Sci.*, 8 (2013) 11492-11501.
22. H. Li, W.Y. Shih and W.H. Shih, *Nanotechnology*, 18 (2007) 205604-205609.
23. R.A. Wessling, *J. Polym. Sci: Polym. Symp.*, 72 (1985) 55-56.
24. D.A. Halliday, P.L. Burn, R.H. Friend, D.D.C. Bradley and A.B. Holme, *Synth. Met.*, 55 (1993) 902-907.
25. C.H. Wu, L.X. Shi, Q.N. Li, H. Jiang, M. Selke, L. Ba and X.M. Wang, *Chem. Res. Toxicol.*, 23 (2010) 82-88.
26. C.X. Li, D.Y. Jiang, L.L. Zhang, J.F. Xia and Q. Qiang, *Langmuir*, 28 (2012) 9729-9734.
27. N. Bhardwaj and S.C. Kundu, *Biotechnol. Adv.*, 28 (2010) 325-347.
28. Y. Xin, Z.H. Huang, P.P. Yang, Z.J. Jiang, C. Wang and C. Shao, *J. Appl. Polym. Sci.*, 114 (2009) 1864-1864.
29. R.S. Johnson, P.S. Finnegan, D.R. Wheeler and S.M. Dirk, *Chem. Commun.*, 47 (2011) 3936-3938.
30. W.L. Yu, H. Zhang, Z.X. Fan, J.H. Zhang, H.T. Wei, D. Zhou, B. Xu, F.H. Li, W.J. Tian and B. Yang, *Energy Environ. Sci.*, 4 (2011) 2831-2834.

31. D.R. Gagnon, J.D. Capistran, F.E. Karasz, R.W. Lenz and S. Antoun, *Polymer*, 28 (1987) 567-573.
32. C. Wang, E.Y. Yan, Z.H. Huang, Q. Zhao and Y. Xin, *Macromol. Rapid Commun.*, 28 (2007) 205-209.
33. M.J. Li, J.H. Zhang, H. Zhang, Y.F. Liu, C.L. Wang, X. Xu, Y. Tang and B. Yang, *Adv. Funct. Mater.*, 17 (2007) 3650-3656.